ISSN 0027-1314, Moscow University Chemistry Bulletin, 2007, Vol. 62, No. 4, pp. 221–225. © Allerton Press, Inc., 2007.
Original Russian Text © A.N. Shatokhin, F.N. Putilin, M.N. Rumyantseva, A.M. Gas'kov, 2007, published in Vestnik Moskovskogo Universiteta. Khimiya, 2007, No. 4, pp. 271–276.

Energy Characteristics and Deposition Rates of Metals from Vacuum Laser Plasma on Dielectric Substrates

A. N. Shatokhin[a], F. N. Putilin[a], M. N. Rumyantseva[b], and A. M. Gas'kov[b]

[a] *Department of Laser Chemistry*
e-mail: shatokhin@laser.chem.msu.ru
[b] *Department of Inorganic Chemistry*
e-mail: roumiantseva@inorg.chem.msu.ru

Received September 11, 2006

Abstract—The effect of the energy flux density of a pulsed Kr–F laser on the processes of generation of the laser plasma of tin, palladium and platinum and on the deposition rates of metal films on dielectric substrates in laser ablation have been studied. The use of the differential scheme of probing a laser plasma with Faraday cups and time-of-flight mass spectrometry has made it possible to distinguish, in plasma ion signals, the ranges of singly charged and multicharged ions, which differ in kinetic energy. The film deposition rate depends on both the laser energy flux density and the degree of ionization of the laser plasma.

DOI: 10.3103/S0027131407040104

The structure and morphology of oxide films deposited by pulsed laser ablation depend mainly on the energy characteristics of laser plasma related to the radiation flux density on the target J [1, 2]. The radiation flux density J is the ratio of the laser pulse energy W to the irradiated target surface area s ($J = W/s$). The flux density can be varied by changing either the laser pulse energy or the area of the focused spot on the target. However, changes in each of these quantities can lead to different changes in the laser plasma characteristics. It was found [3] that a proportional increase in the area and energy, the J value being unaltered, has a considerable effect on the energy spectrum of laser plasma ions, which is due to an increase in the region of interaction between the laser radiation and the laser plasma itself. To prevent this effect, in this work, the flux density was varied by changing the laser pulse energy with a minimal area of the focused spot on the target being retained.

The plasma of a compound deposited by pulsed laser ablation is usually sufficiently ionized to be studied by Langmuir probes [4, 5]. These measurements make it possible to estimate the kinetic energies and concentration of singly charged particles and the plasma temperature. However, as applied to a stationary equilibrium plasma, interpretation of the current–voltage curves obtained with such probes is rather ambiguous and depends on the parameters of both the probe and the plasma to be studied [5]. A major distinction of a nonstationary pulsed laser plasma is the ordered motion of differently charged particles whose concentrations and velocities vary in time and space. This can lead to false signals related to displacement currents, secondary particle emission, and impact ionization of highly excited atoms impinging on the surface of a probe collector [4]. To prevent, insofar as possible, these interferences, we used screened grid probes of the Faraday cup type with a biased collector oriented normally to the direction of plasma propagation [5]. In addition, a differential scheme of measuring the plasma spread velocities by two identical probes located at different distances from the target were used, which eliminates the errors caused by the uncertainty of the plasma pulse onset and duration with respect to the laser pulse for different radiation energies [6, 7]. The charge multiplicity in the laser plasma was determined by time-of-flight mass spectrometry [8, 9]: changes in the velocity of different charges passing through an electric field generated by parallel grid electrodes were recorded.

EXPERIMENTAL

The scheme of the experimental setup and main devices—an excimer pulsed Kr–F laser, a vacuum chamber, and an optical system that focuses the laser beam on targets—were described in detail in [2, 7, 10]. Instrumentation for differential probe measurements was described in [6, 11]. In the present work, targets were plates made of tin (10 mm in diameter and 3 mm in thickness), palladium ($10 \times 10 \times 0.5$ mm), and platinum ($10 \times 10 \times 1$ mm). Metals for all targets had a purity of 99.9999%. The pressure in the vacuum chamber during experimental runs was maintained at the level $p = 10^{-3}$ Pa. The laser pulse energy was varied by controlling the voltage on the discharge circuit of laser pumping.

To determine the energy flux densities, the pulse energy and the area of the focused spot on the target

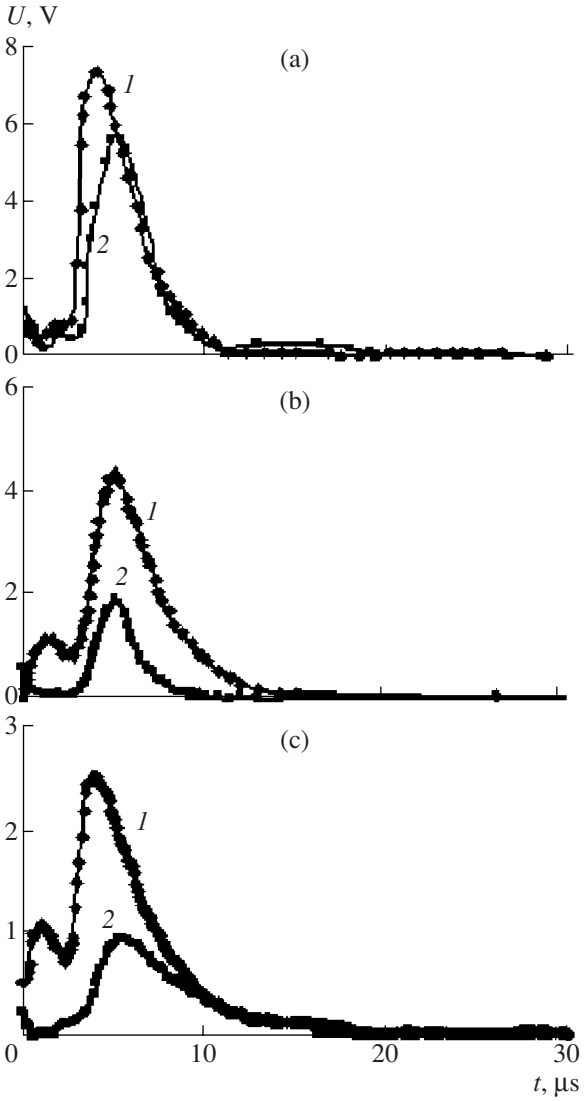

Fig. 1. Signals for the (*1*) nearby and (*2*) distant probes (Δr = 4 cm) in a palladium laser plasma at energy flux densities of (a) 80, (b) 40, and (c) 20 J/cm^2.

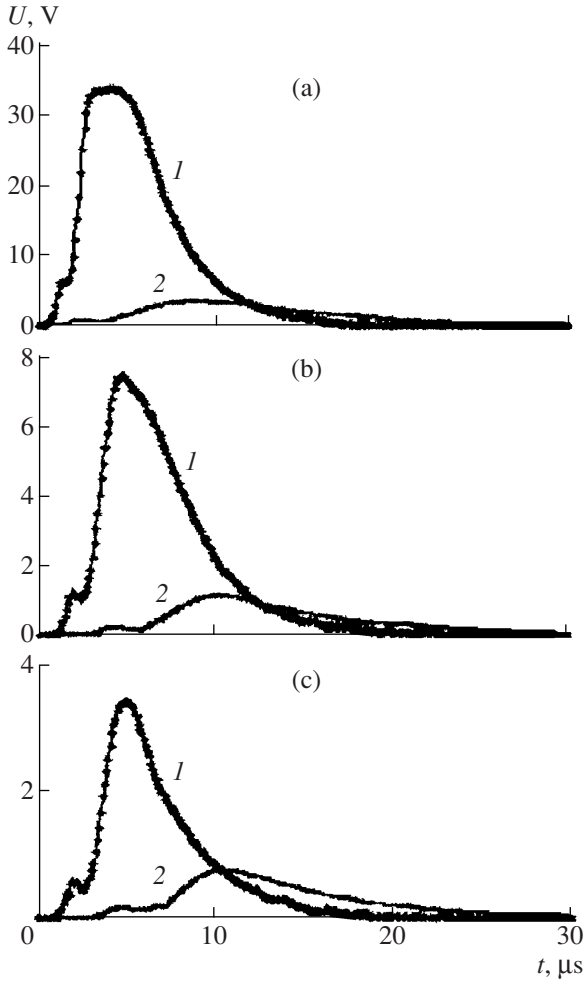

Fig. 2. Signals for the (*1*) nearby (U_{10}) and (*2*) distant (U_{20}) probes (Δr = 7 cm) in a platinum laser plasma at energy flux densities of (a) 80, (b) 40, and (c) 20 J/cm^2.

should be known. In preliminary experiments, we demonstrated that the size of the ablation crater formed on polished metal targets by a sharply focused laser beam depends on the pulse energy. The crater sizes were measured by an IZA-2 microscope and a Talystep profilometer on fixed targets exposed to 20-pulse trains. These measurements showed that, at high ablation thresholds, the crater area can be approximated using a least-squares procedure by the linear function $s(W) = kW + 0.12$ (mm^2) with an accuracy of 5%. Inasmuch as the minimal energies at which a crater can form on the surface are determined by the laser ablation thresholds ($W > 0$), which depend on the electrophysical properties of the target material [6, 12], the true geometric size of the focused spot area can be determined by extrapolation of the experimental plot to the value $W = 0$: $s(0) = 0.12$ mm^2. Thus, the energy flux density was calculated by the formula $J = 10^4 W/12$ (J cm^{-2}).

The probes were located at different distances (r_1, r_2) from the target but at the same angles in the plane near the normal to the ablation zone in order to avoid shielding of a probe by the other one. Figures 1 and 2 show the signals of the nearby and distant probes for different energy flux densities on the targets corresponding to the ion currents of palladium and platinum.

Comparison of the signals of probes 1 and 2 (Figs. 1 and 2) shows that, while the signal is recorded, the particle velocity changes from maximum to minimum since the corresponding time lag between the arrivals of charges at the probes increases from minimum to maximum. On the one hand, ion currents can be calculated by the Ohm law from the voltage drop induced by charged particles at the output resistors of the probe collectors (R = 1 kΩ). On the other hand, the current induced by charges moving in space is determined as

the derivative of the charge q with respect to the time t at the point r of space [6, 12]:

$$I(t) = dq/dt = (dq/dr)(dr/dt) = \rho_q(t)V(t), \quad (1)$$

where $\rho_q(t)$ is the linear charge density, and $V(t)$ is the charge velocity.

Signal processing and calculations of the ion velocity–energy spectra were performed based on the numerical solution of Eqs. (1)–(4):

$$I_{2n}(t) = I_2(t)\frac{\int_0^{+\infty} I_1(t)dt}{\int_0^{+\infty} I_2(t)dt}, \quad (2)$$

$$\int_0^t I_1(x, r)dx = \int_0^{t+\tau} I_{2n}(y, r + \Delta r)dy, \quad (3)$$

$$V_i(t) = \frac{\Delta r}{\tau(t, \Delta r)}. \quad (4)$$

Here, I_1 and I_2 are the ion currents of probes 1 and 2, respectively; Eq. (2) is the condition of normalization of the ion current of probe 2 to the current of probe 1; I_{2n} are the normalized currents of probe 2; Eq. (3) is for calculation of the time delay τ between the arrivals of equal integral charges at the probes; Eq. (4) is for calculation of the velocities, which are substituted into Eq. (1) to obtain the charge distribution density, $\Delta r = r_2 - r_1$. Equations (1)–(4) make it possible to calculate not only the velocity and, thus, energy spectra of ions which are usually obtained by means of time-of-flight mass spectrometric studies of laser plasma [8, 9], but also time-dependent instantaneous spectra [6]. To determine the charge multiplicity by means of a linear electrostatic mass spectrometer, a grounded screening grid was placed between the target and the first probe, and accelerating (decelerating) grids with the same potential U with respect to the ground were placed behind the first and the second probes. Thus, the more distant probe is in the region of the drift of charged plasma particles. Comparison of the changes in the time of detection by the probes of the ion currents in the leading and falling edges of ion signals and calculation of velocities for potentials of different magnitude and polarity on the grids made it possible to calculate the charge multiplicities (k_i) of ions relative to the elementary charge (q_e) by the formula [8, 9]

$$\frac{M}{2}\left|V_i^2 - V_{0i}^2\right| = k_i q_e |U|, \quad (5)$$

where M is the ion mass, V_{0i} is the ion velocity in the absence of an external electric field, and V_i is the ion velocity modified by an external electric field of voltage U.

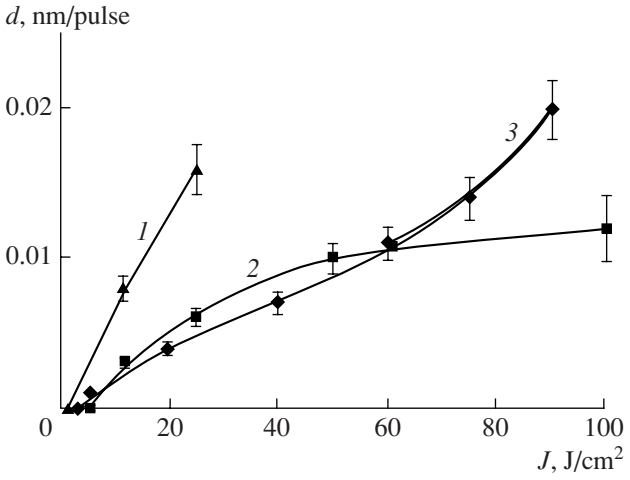

Fig. 3. Pd, Pt, and Sn film thickness (per pulse) as a function of the energy flux density of the Kr–F laser.

The calculated charge multiplicity for the leading edge of the ion current, $k_1 = 1.9$, is close to 2, and that for the falling edge, $k_2 = 0.9$, is close to 1. This can be accepted as a good approximation, taking into account that Eq. (5) implies the existence of a homogeneous electric field between the screening and accelerating grids, which is the case only for a field between infinite parallel planar conductors, with no other conductors between them [8]. At the same time, these calculations did not reveal, in the probe signals of laser plasma ion currents, the presence of charged clusters with masses multiple of the masses of metal atoms.

To determine the mass loss of the targets in ablation and metal film thicknesses as a function of the energy flux density, substrates made of polished oxidized silicon, glass ceramics, or polycor were mounted parallel to the target at the place corresponding to the maximum of the metal deposition surface density. The substrates were fixed at a distance of 4 cm from the target in a holder, behind which a tungsten coil electric heater in a quartz tube was located. Metal deposition was carried out through a mask with a 4×8 mm window applied to the substrate surface. Prior to laser ablation of the targets, the masked substrates were degassed by heating them to 240°C in a vacuum for 1 h and then were cooled in a vacuum for 1 h. In these experiments, the laser pulse frequency was 500 pulses/min (~8.3 Hz). The laser ablation duration was varied to achieve the necessary accuracy of measuring film thicknesses on a profilometer and weighing target mass losses on an analytical balance. The results of these runs are presented in the table and Fig. 3. For tin films, the thickness data are limited by the energy flux energy $J \sim 25$ J/cm^2 (for Pt and Pd, $J \sim 100$ J/cm^2) since, under the constant focusing conditions used, a further increase in J causes the appearance of plasma particles of uncontrollable size, which impairs the accuracy of measurements of deposited film thicknesses and target mass losses (for tin tar-

Table

Target	Energy flux density, J/cm^2	Number of pulses	Target mass loss, mg	Average film thickness, nm	Target mass loss per pulse, g/pulse	Film thickness per pulse, nm/pulse
Pd	20	7500	0.5	30	0.7×10^{-7}	4×10^{-3}
	40	7500	0.9	55	1.2×10^{-7}	7×10^{-3}
	60	7500	1.4	85	2.1×10^{-7}	11×10^{-3}
	80	5000	1.6	95	3.2×10^{-7}	14×10^{-3}
	100	5000	–	110	–	20×10^{-3}
Pt	12	10000	0.9	30	0.9×10^{-7}	3×10^{-3}
	25	10000	2	60	2×10^{-7}	6×10^{-3}
	50	7500	2.9	75	3.9×10^{-7}	10×10^{-3}
	100	5000	–	60	–	12×10^{-3}
Sn	12	10000	–	70	–	7×10^{-3}
	25	10000	–	160	–	16×10^{-3}

gets, this is also due to their large initial masses). The minimal energy densities for zero film thicknesses in Fig. 3 were obtained from probe measurements of target ablation thresholds [6]. The lines in Fig. 3, drawn using the Excel program, approximate the experimental values by third-order polynomials.

RESULTS AND DISCUSSION

In the energy flux density range 10–50 J/cm^2 for Pt films (up to 80 J/cm^2 for Pd), the film deposition rates are directly proportional to the target mass loss and the energy flux density (table, Fig. 3).

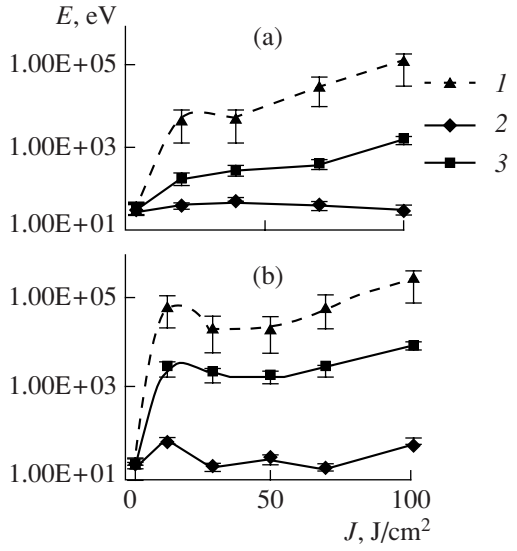

Fig. 4. Limits of changes in the kinetic energy of singly charged (Pt^+ and Pd^+) and multicharged (Pt^{n+} and Pd^{n+}) ions of the platinum and palladium laser plasma as a function of the energy flux density of the Kr–F laser on the targets.

At r = 4 cm, the surface atom distribution densities per laser ablation pulse as a function of the energy flux density were calculated from the experimental data on film thicknesses (deposition rates), the tabulated mass volume densities of the metals and their atomic masses, and the Avogadro number [13]. For palladium,

$$N_{0s}^{Pd}(J) = (0.56J + 30.1) \times 10^{12} \text{ at/pulse cm}^2. \quad (6)$$

For platinum,

$$N_{0s}^{Pt}(J) = (0.62J + 80.1) \times 10^{12} \text{ at/pulse cm}^2. \quad (7)$$

Here, $N_{0s}^{M}(J, r)$ is the surface distribution density of atoms on the substrate located at the distance r from the target along the normal to the ablation zone.

Figure 4 shows the limits of the change in the kinetic energies of Pt and Pd ions calculated from the experimental dependences of ion currents on time and energy flux density on the target. The ranges of singly charged and multicharged ions are shown. As is seen, the maximal kinetic energies of ions of the corresponding multiplicity for palladium are higher than for platinum. In the energy flux density range ~10–80 J/cm^2, the kinetic energies of palladium ions are constant (within the error of measurements). They increase only in the ranges from the ablation threshold to 10 J/cm^2 and from 80 to 100 J/cm^2. The maximal kinetic energies of platinum ions increase over the entire range studied, from the ablation threshold to 100 J/cm^2.

Noteworthy are the differences in the degree of ionization of the Pd and Pt plasmas, which can be calculated from the ratio of integral ion charge densities on the probe collectors recalculated to the distance to the target (4 cm) to the surface atom distribution densities (6) and (7). These calculations show that the degree ionization of the metal plasma increases with an increase in the energy flux density from 10 to 80 J/cm^2. The degree of ionization of the laser plasma for Pt (3.2–

21.6%) is higher than that for Pd (2.8–5.4%), despite the relatively lower content of multiply ionized atoms (compare the ion current amplitudes in Figs. 1 and 2).

This can account for the different dependences of the film deposition rates of Pd and Pt on substrates (Fig. 3). The platinum film deposition rate can decrease at large energy densities due to an increase in the effect of surface sputtering by high-velocity ions. This effect was also observed in [14] upon vacuum-arc plasma deposition of platinum on substrates.

REFERENCES

1. Kwok, H.S., Kim, H.S., Kim, D.H., et al., *Appl. Surf. Sci.*, 1997, vols. 109–110, p. 595.
2. Shatokhin, A.N., Putilin, F.N., Ryzhikov, A.S., et al., *Sensor*, 2003, nos. 3–4 (9), p. 38.
3. Bykovskii, Yu.A. and Nevolin, Yu.N., *Lazernaya mass-spektrometriya* (Laser Mass Spectrometry), Moscow, 1985.
4. Babenko, A.N., Kruglyakov, E.P., Kurtmullaev, R.Kh., et al., in *Diagnostika plazmy* (Plasma Diadnostics), Moscow, issue 3, 1973.
5. *Plasma Diagnostics*, Lochte-Holtgreven, W., Ed., Amsterdam: North-Holland, 1968. Translated under the title *Metody issledovaniya plazmy*, Moscow: Mir, 1971.
6. Shatokhin, A.N., Demidov, A.V., Putilin, F.N., et al., *Vestn. Mosk. Univ., Ser. 2. Khim.*, 2001, vol. 42, p. 167.
7. Shatokhin, A.N., Safonova, O.V., Putilin, F.N., et al., *Neorg. Mater*, 2002, vol. 38, p. 462.
8. Rik, G.R., *Mass-spektroskopiya* (Mass Spectroscopy), Moscow, 1953.
9. Stoian, R., Varel, H., Rosenfeld, A., et al., *Appl. Surf. Sci.*, 2000, vol. 165, p. 44.
10. Morozova, N.V., Gas'kov, A.M., Kuznetsova, T.A., et al., *Neorg. Mater*, 1996, vol. 32, p. 326.
11. Shatokhin, A.N., Kudryashov, S.I., Safonova, O.V., et al., *Khim. Vys. Energ.*, 2000, vol. 34, p. 219.
12. Ready, J.F., *Effects of High-Power Laser Radiation*, New York: Academic, 1971. Translated under the title *Deistvie moshchnogo lazernogo izlucheniya*, Moscow, Mir, 1974.
13. *Fizicheskie velichiny* (Physical Quantities), Grigor'ev, I.S. and Meilikhov, E.Z., Eds., Moscow, 1991.
14. Avrekh, M., Monteiro, O.R., and Brown, I.G., *Appl. Surf. Sci.*, 2000, vol. 158, p. 217.